Search for non-resonant di-Higgs production in the $HH \to b\bar{b}\gamma\gamma$ decay channel in pp collisions at $\sqrt{s} = 13$ TeV with the ATLAS experiment

Alex Wang (University of Wisconsin-Madison)

On behalf of the ATLAS collaboration, LHCP2021

Introduction

- Since the discovery of the Higgs boson, one of the goals of LHC physics has been to observe di-Higgs (HH) production as a probe of the Higgs boson self-coupling.
- At 13 TeV, non-resonant di-Higgs production proceeds mainly through gluon-fusion (ggF) from two leading order diagrams.

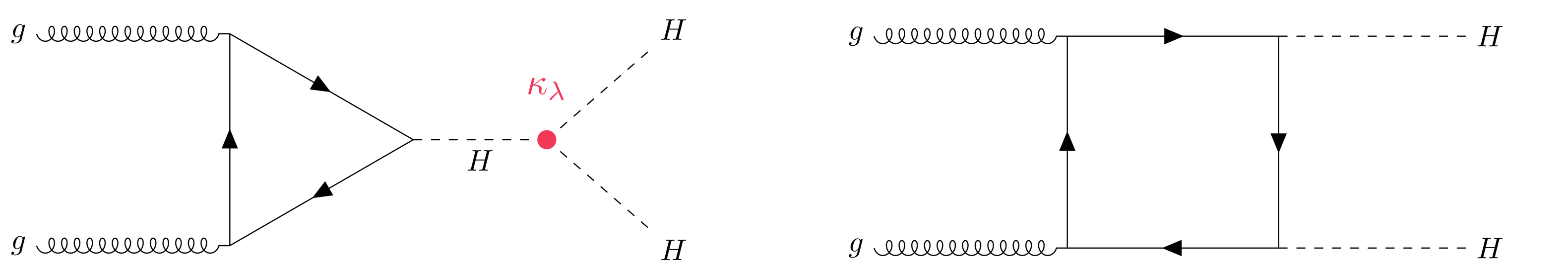

Figure 1: Leading order diagrams for HH ggF production.

- In the SM, these diagrams interfere destructively and lead to a small production cross-section of 31 fb.
- BSM modifications to the self-coupling $\kappa_\lambda = \lambda_{HHH}/\lambda_{HHH}^{SM}$ can result in much higher cross-sections.
- The cross-section from vector-boson fusion (VBF) is also considered but is much smaller (1.7 fb in the SM).

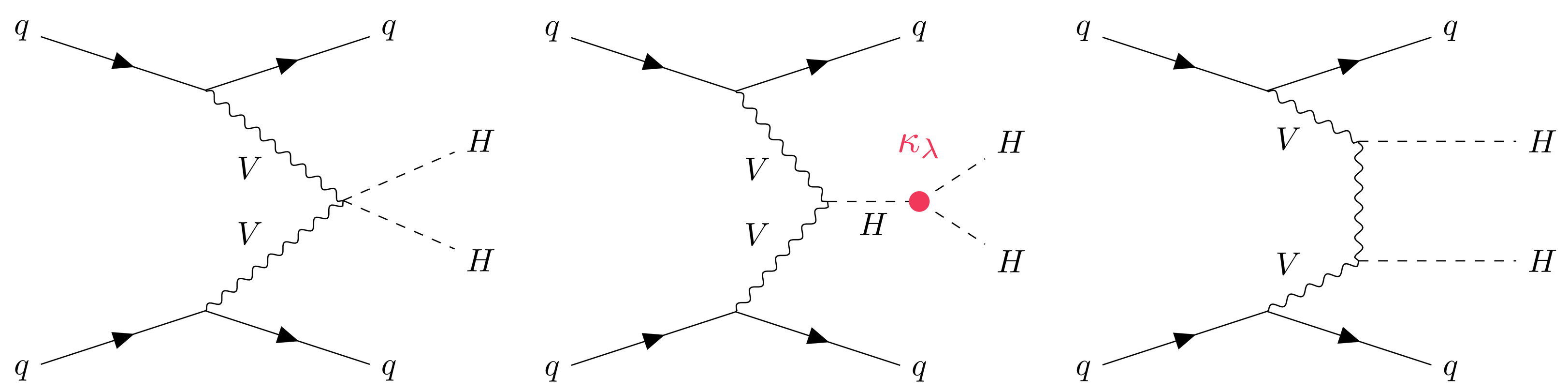

Figure 2: Leading order diagrams for HH VBF production.

- The $HH \to b\bar{b}\gamma\gamma$ channel is one of the most sensitive to HH production.
- It combines the large $H \to bb$ branching ratio with the excellent ATLAS $H \to \gamma\gamma$ mass resolution.
- The latest $HH \to b\bar{b}\gamma\gamma$ result (ATLAS-CONF-2021-016) uses the full ATLAS Run 2 dataset of 139 fb^{-1} to search for non-resonant HH production.

See the results!

Analysis Strategy

- Events with two photons and two b-jets are selected.
- Events are divided into a high mass (targeting SM-like signals) and low mass region (targeting non SM-like signals) using the modified 4-body mass $m^*_{b\bar{b}\gamma\gamma} = m_{b\bar{b}\gamma\gamma} - (m_{b\bar{b}} - 125\ \mathrm{GeV}) - (m_{\gamma\gamma} - 125\ \mathrm{GeV})$.

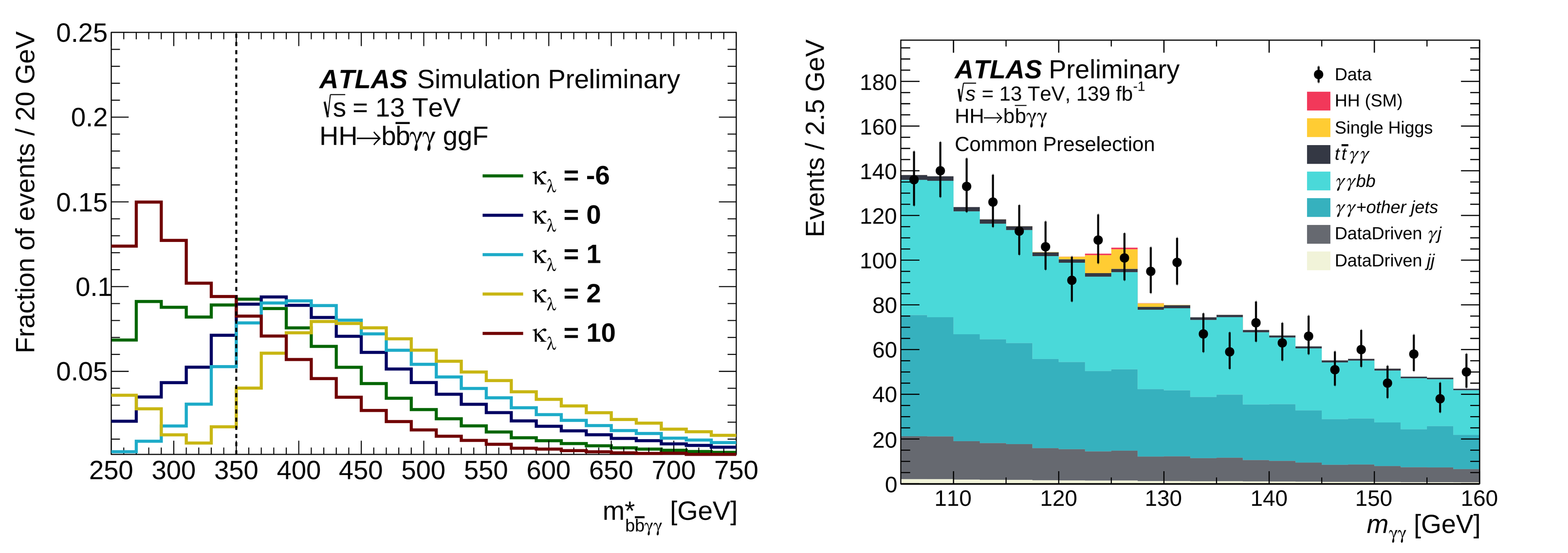

Figure 3: The $m^*_{b\bar{b}\gamma\gamma}$ distribution for various HH signals (left) and the expected $m_{\gamma\gamma}$ composition for signals and backgrounds (right).

- The main backgrounds include non-resonant $\gamma\gamma$ events and single Higgs from $H \to \gamma\gamma$ (ggF, VBF, $t\bar{t}H$).
- In each mass region a boosted decision tree (BDT) is trained to separate the HH signal from the backgrounds.
- The training uses kinematic variables related to the photons and jets such as $m_{b\bar{b}}$ and $p_T^\gamma/m_{\gamma\gamma}$.

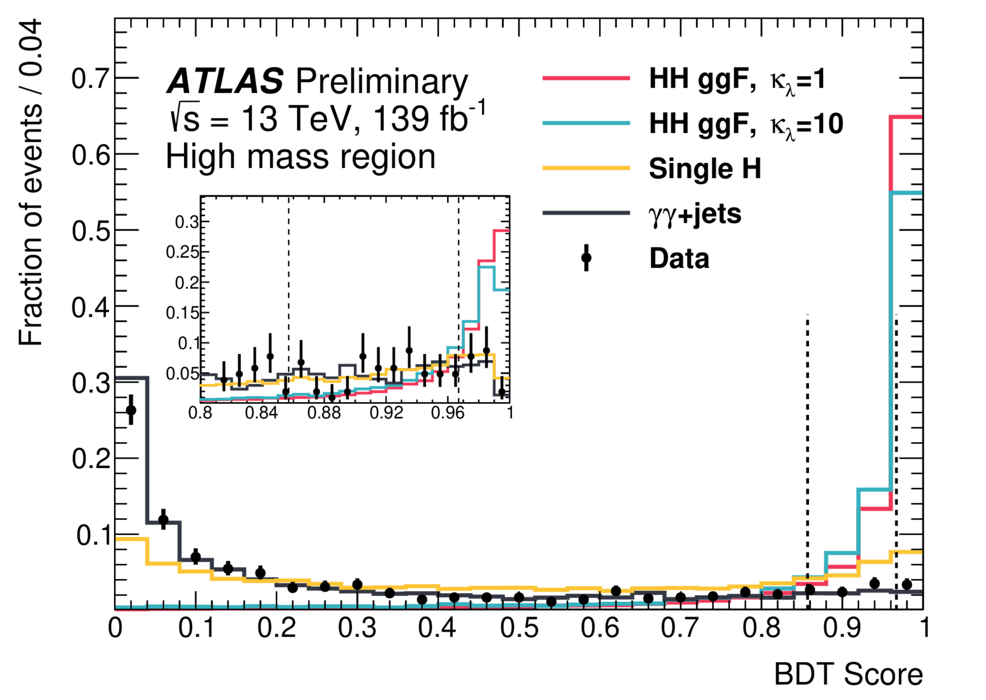

Figure 4: The BDT distribution of the HH ggF signal in the high mass region.

- A total of 4 signal sensitive categories are created using the BDT outputs.

Analysis Results

- The HH signal is obtained from a simultaneous fit to the diphoton mass spectrum $m_{\gamma\gamma}$ across all categories.
- No significant excess is observed and upper limits are set at 95% CL.

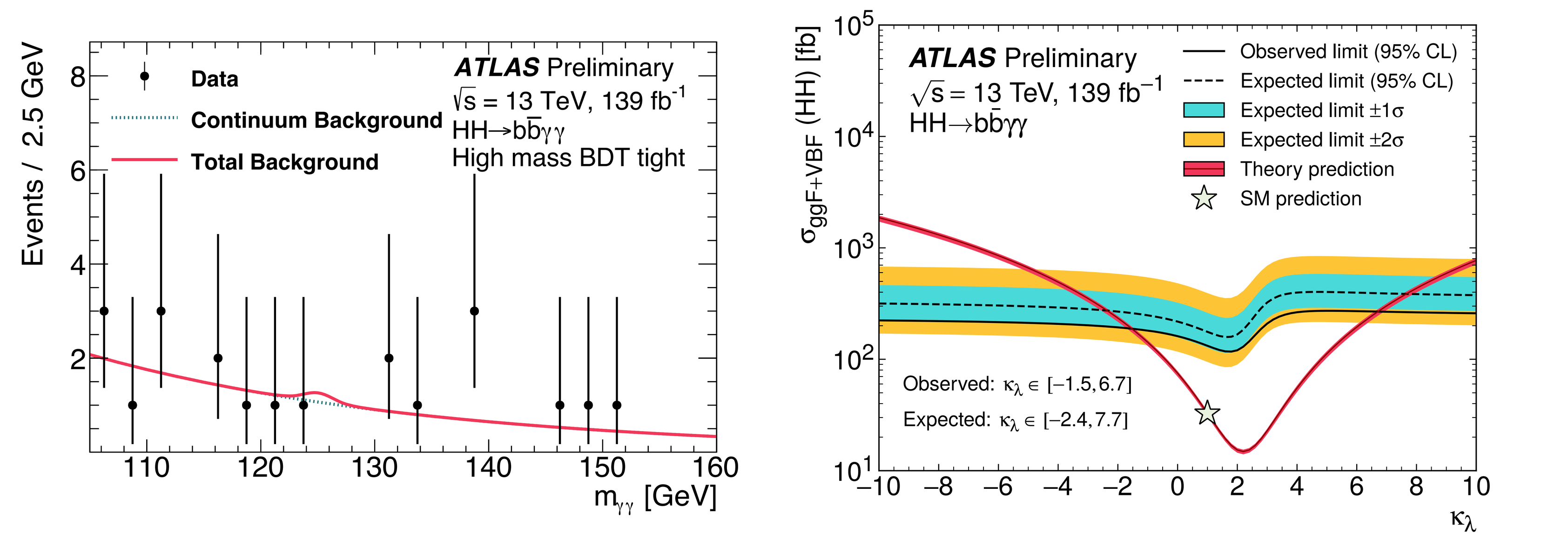

Figure 5: The fitted diphoton mass spectrum from the most sensitive category in the high mass region (left) and the HH cross-section limits as a function of κ_λ (right).

- The observed (expected) limit on the HH non-resonant production cross-section is 130 fb (180 fb).
- This corresponds to 4.1 (5.5) times the SM cross-section.
- The observed (expected) constraint on the Higgs boson self-coupling is $-1.5 < \kappa_\lambda < 6.7$ ($-2.4 < \kappa_\lambda < 7.7$).
- Compared to the previous 36 fb^{-1} analysis, the new results improve the SM cross-section limit by a factor of 5 and the allowed κ_λ range by a factor of 2.

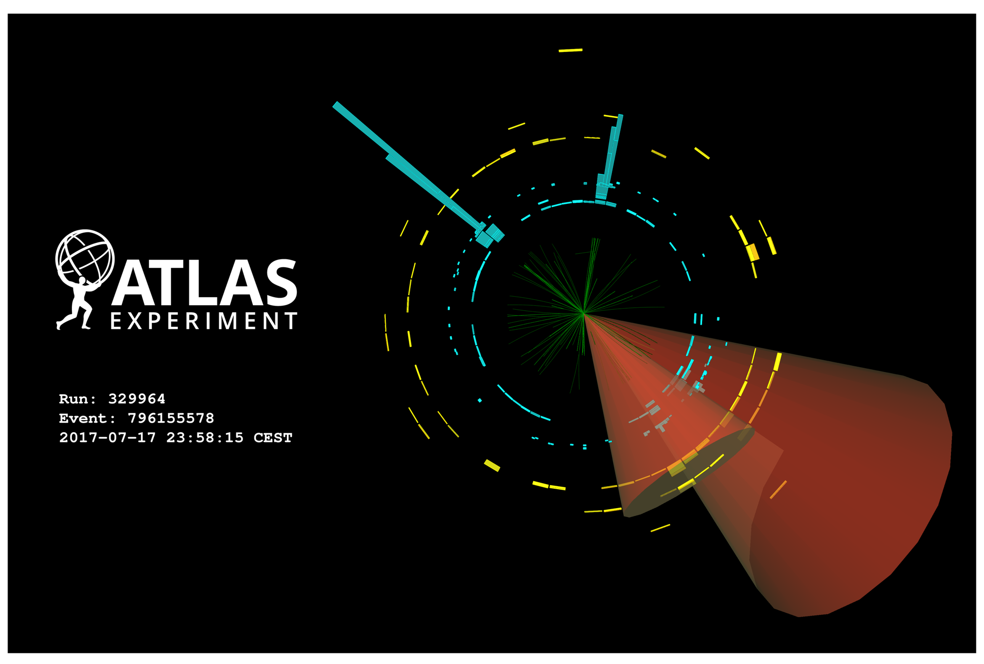

Figure 6: A candidate $HH \to b\bar{b}\gamma\gamma$ event, showing two b-jets (red cones) with an invariant mass of $113\ \mathrm{GeV}$ and two photons (cyan towers) with an invariant mass of $123\ \mathrm{GeV}$.